

THESIS FOR THE DEGREE OF LICENTIATE OF ENGINEERING

Characterization of Microwave Transistors for Robust
Receivers and High Efficiency Transmitters

MATTIAS THORSELL



Microwave Electronics Laboratory
Department of Microtechnology and Nanoscience (MC2)
Chalmers University of Technology
Göteborg, Sweden, 2009

Characterization of Microwave Transistors for Robust Receivers and High Efficiency Transmitters

MATTIAS THORSELL

© Mattias Thorsell, 2009.

Chalmers University of Technology
Department of Microtechnology and Nanoscience (MC2)
Microwave Electronics Laboratory
SE-412 96 Göteborg, Sweden
Phone: +46 (0) 31 772 1000

Technical report MC2-139
ISSN 1652-0769

Printed by Chalmers Reproservice
Göteborg, Sweden 2009

Abstract

The next generation of integrated transceiver front-ends needs both robust low noise amplifiers and high power amplifiers on a single-chip. The Aluminium Gallium Nitride / Gallium Nitride (AlGaN/GaN) High Electron Mobility Transistors (HEMT) is a suitable semiconductor technology for this purpose due to its high breakdown voltage and high electron mobility. In this thesis the AlGaN/GaN HEMT's thermal properties, noise and survivability have been characterized for the intended use in robust high power transceivers. Furthermore, a new characterization setup for load modulated high efficiency power amplifiers have been developed.

The thermal properties of AlGaN/GaN HEMTs have been carefully investigated considering self-heating and its effect on small-signal parameters and high frequency noise. Self-heating is a severe problem for a high power transistor on any semiconductor material, including GaN. In addition to reliability problems, the performance of the operating HEMT degrades with temperature. The access resistances showed a large temperature dependence, which was also verified with TLM measurements. Due to the large self-heating, the temperature dependence of the access resistances has to be taken into account in the modeling of the AlGaN/GaN HEMT. A temperature dependent small-signal noise model was derived and verified through fabricated amplifiers. Design strategies for robust low noise amplifiers are discussed and implemented using the derived model.

The new characterization setup gives new possibilities to characterize the performance of load modulated amplifiers. Recent results on load modulated amplifiers show promising efficiency improvements in back-off operation. Therefore a new measurement setup was developed that performs dynamic load modulation at the transistor terminals. This method should be useful to further improve the performance of load modulated amplifiers for high efficiency operation. The measurement setup is based on an active load-pull setup, where a modulated input signal is used to synthesize a time varying output power. The load impedance is dynamically controlled with the envelope of the input signal, following an optimum efficiency load trajectory. This gives better insight into device operation and possible improvements.

Keywords: AlGaN/GaN HEMT, thermal characterization, self-heating, access resistance, noise modeling, active load-pull, load modulation

List of Publications

Appended Publications

This thesis is based on work contained in the following papers:

- [A] M. Thorsell, K. Andersson, M. Fagerlind, M. Södow, P.-Å. Nilsson, and N. Rorsman "Thermal Study of the High-Frequency Noise in GaN HEMTs," in *IEEE Transactions on Microwave Theory and Techniques*, vol. 57, no. 1, pp. 19–26, 2009.
- [B] M. Thorsell, K. Andersson, M. Fagerlind, M. Södow, P.-Å. Nilsson, and N. Rorsman "Characterization of the temperature dependent access resistances in AlGa_N/Ga_N HEMTs," in *2008 Workshop on Integrated Nonlinear Microwave and Millimetre-Wave Circuits*, Malaga, Spain, 2008, pp. 17–20.
- [C] M. Thorsell, K. Andersson, and C. Fager "Characterization Setup for Device Level Dynamic Load Modulation Measurements," to appear in *2009 IEEE MTT-S International Microwave Symposium Digest*, Boston, MA, USA, 2009.
- [D] M. Södow, M. Fagerlind, M. Thorsell, K. Andersson, N. Billström, P.-Å. Nilsson, and N. Rorsman "An AlGa_N/Ga_N HEMT-Based Microstrip MMIC Process for Advanced Transceiver Design," in *IEEE Transactions on Microwave Theory and Techniques*, vol. 56, no. 8, pp. 1827–1833, 2008.

Other Publications

The following papers have been published but are not included in the thesis. Their content partially overlap with the appended papers or are out of the scope of this thesis.

- [a] M. Thorsell, K. Andersson, M. Fagerlind, M. Südow, P.-Å. Nilsson, and N. Rorsman "Thermal characterization of the intrinsic noise parameters for AlGaN/GaN HEMTs," in *2008 IEEE MTT-S International Microwave Symposium Digest*, Atlanta, GA, USA, 2008, pp. 463–466.
- [b] M. Südow, H.M. Nemati, M. Thorsell, U. Gustavsson, K. Andersson, C. Fager, P.-Å. Nilsson, J. Hassan, A. Henry, E. Janzen, R. Jos, and N. Rorsman "SiC Varactors for Dynamic Load Modulation of High Power Amplifiers," in *IEEE Electron Device Letter*, vol. 29, no. 7, pp. 728–730, 2008.
- [c] M. Südow, K. Andersson, M. Fagerlind, M. Thorsell, P.-Å. Nilsson, and N. Rorsman "A Single-Ended Resistive X-Band AlGaN/GaN HEMT MMIC Mixer," in *IEEE Transactions on Microwave Theory and Techniques*, vol. 56, no. 10, pp. 2201–2206, 2008.

Contents

Abstract	iii
List of Publications	v
1 Introduction	1
1.1 GaN transceivers	2
1.2 Wireless communications	4
2 Thermal measurements	7
2.1 Self-heating	7
2.2 Access resistances	8
2.3 Intrinsic model parameters	11
3 Noise characterization and modeling	15
3.1 Noise parameter characterization	15
3.2 Noise modeling	16
3.3 Design of robust LNA	19
4 Dynamic load-pull	23
4.1 Active load-pull setup	23
4.2 Load modulation	24
4.3 Dynamic load modulation characterization	25
5 Conclusions	27
5.1 Future work	27
Acknowledgments	29
Bibliography	31

Chapter 1

Introduction

The interest for Aluminium Gallium Nitride / Gallium Nitride (AlGaN/GaN) High Electron Mobility Transistors (HEMT) has increased rapidly during recent years. A decade ago the GaN HEMT¹ was only available in the research labs, showing promising results in terms of breakdown, power density and efficiency. These results indicated that the GaN HEMT could fulfill the high demands that future wireless communication and radar systems have on microwave transistors. The large need for high performing transistors in microwave systems have lead to that several commercial suppliers today claim to deliver high power GaN HEMTs with excellent performance².

The material properties of GaN are outstanding compared to other commonly available semiconductors. This is partially due to that GaN is a wide bandgap material, thus it has a high breakdown field. Another benefit with GaN is the possibility to grow a HEMT structure. The high mobility, due to the HEMT structure, makes it suitable for high frequency and low noise applications. Another interesting wide bandgap semiconductor is silicon carbide (SiC). While it has high breakdown field, it has not yet been possible to fabricate a HEMT structure on SiC. Therefore SiC is probably not the best candidate for high frequency and low noise applications. The most important material parameters for GaN and other semiconductor materials are listed in Table 1.1.

Table 1.1: Material properties [1,2]

	Si	GaAs	InP	4H-SiC	GaN
E_g (eV)	1.1	1.42	1.34	3.26	3.39
μ_e (cm ² /Vs)	1350	8500	5400	700	2000 [2DEG]
E_{br} (MV/cm)	0.3	0.4	0.5	3.0	3.3
k (W/cm K)	1.5	0.43	0.68	3.3-4.5	1.3

The GaN HEMT is an excellent transistor for high power amplifiers (HPA). This is due to its high voltage and high current operation, resulting in a

¹GaN HEMT hereafter refers to HEMT structures based on GaN

²Some available commercial suppliers: Cree Inc, Nitronex Corporation and Eudyna Devices Inc.

high power density, thus reducing the die size for a fixed output power. The high operating voltage of the GaN HEMT also provides the possibility to obtain high output power with higher load impedance, thus simplifying the output matching. Overall this makes it possible to obtain high power and high efficiency with a GaN amplifier.

The GaN HEMT have shown very high power densities of up to 40 W/mm [3]. The dissipated power could therefore be very high for a small surface area. For example, the maximum theoretical efficiency for a class B amplifier is 78 %. Hence, for an amplifier with 100 W delivered output power, additionally at least 28 W is dissipated as heat. This increases the demands on efficient heat conduction. In Table 1.1 it is shown that the thermal conductivity of GaN is roughly the same as for Si. The self-heating for a GaN HEMT is therefore significantly higher than for a Si LDMOS with the same output power, due to the higher power density. GaN is usually grown on a substrate. By choosing a substrate with high thermal conductivity, such as SiC, the self-heating effect is partly reduced. It has also been shown that the nucleation layer between the substrate and the GaN material has a large influence on the thermal resistance [4]. However, for HEMT structures grown on Sapphire, Si or free standing GaN-films the self-heating is of major concern.

High temperature is well know to accelerate transistor degradation, thus accelerated median time to failure (MTTF) test are carried out to specify reliability [5]. Channel temperatures (T_{CH}) reaching far beyond 300 °C are reported for high power GaN transistors [6]. Self-heating does not only reduce lifetime, but it also degrades the performance. The large increase in the channel temperature decreases the electron mobility [7], thus increasing the access resistances [A]. The self-heating and its effects on the access resistances and the intrinsic small-signal parameters are therefore thoroughly studied in Chapter 2.

1.1 GaN transceivers

Transceivers used for radar applications need both high output power and robust low noise amplifiers. The GaN HEMT could possibly fulfill both of these demands due to the high breakdown voltage and high electron mobility. The robustness of the GaN HEMT was studied in [8]. Depending on the drain bias the survivability was limited either by the gate current or channel breakdown. For low drain bias, the limiting effect was the rapid increase in gate current with increased input power. This failure mechanism was verified in [9] with large-signal measurements. The gate current was the critical factor for survivability and channel breakdown was not observed. The robustness was improved by introducing a series resistor in the gate dc feed, hence the gate current was decreased significantly due to the voltage drop over the resistor. This improvement in survivability was also shown in [10], where a 8-11 GHz LNA survived input powers up to 41 dBm (pulsed). In [11] the survivability of a 2-12 GHz LNA was measured and no degradation in performance was observed when stressed with input power of 46 dBm (pulsed).

Due to the nature of HEMTs, the GaN HEMT have high electron mobility and therefore low parasitic resistances. Minimum noise figures (F_{min}) less

Table 1.2: Reported GaN LNAs

Frequency [GHz]	F_N [dB]	$ S_{21} $ [dB]	
1 - 9	2	15	[14]
2 - 8	0.9	6	[15]
4 - 7	1	12	[16]
4 - 12	2	15	[10]
5 - 7	1.8	20	[9]
8 - 12	2	10	[12]

than 1 dB have been reported in [8, 12, 13] with more than 10 dB of available gain at X-band (8-12 GHz). This makes GaN HEMTs very suitable for low noise applications. Several LNAs have been reported showing excellent low noise performance at room temperature, Table 1.2.

The GaN key figures: high power density, high efficiency, robustness and good low noise performance opens up new possibilities in radar transceiver design. Complete transceiver monolithic integrated microwave circuits (MMIC) in GaN are possible to manufacture and could outperform available solutions in GaAs due to the survivability of the LNA. GaAs LNAs have only survived up to 26 dBm of input power [17]. In order to improve the robustness, a limiter is used for GaAs receivers. The limiter significantly degrades the low noise performance of the receiver. Typically the limiter loss is at least 1 dB at X-band [18], which degrades the low noise performance with at least 1 dB. Reported F_{min} for InGaAs HEMTs at X-band is below 0.6 dB [19]. Thus the overall receiver noise figure with a typical PIN-limiter for protection is at least 1.6 dB. This should be compared to GaN HEMTs with reported F_{min} below 1 dB at X-band, surviving more than 40 dBm of input power. In [20], a multi-chip X-band GaN transceiver front-end is presented with an output power of 43 dBm and a noise figure of 1.5 dB. The robustness, low system noise figure, together with excellent output power performance makes the GaN HEMT an excellent candidate for transceiver MMICs.

The possibility to make a single-chip solution with GaN is a major benefit. Available GaAs transceiver front-ends consists of at least HPA, limiter, LNA, and circulator or switch, as illustrated Fig. 1.1. The manufacturing and assembling cost of multi-chip solutions is significantly higher than for single-chip solutions, thus motivating the more expensive GaN MMIC.

The reduced number of chips also reduces sensitive and performance degrading interconnects which needs to be accurately modeled for optimum performance. A single chip GaN transceiver MMIC also benefits from smaller dimensions than traditional multi-chip solutions. This is an important advantage for airborne systems where size and weight needs to be reduced. Such a system would allow new solutions for airborne phased array antennas with the possibility to integrate the transceiver with the antenna, further reducing lossy interconnects.

A transceiver is often operated at elevated temperatures partly due to the HPA, but also due to other electronics and inadequate cooling. The large self-heating of GaN HEMTs is a possible problem for single-chip transceivers. The HPA and the LNA are in close proximity of each other, thus increasing the

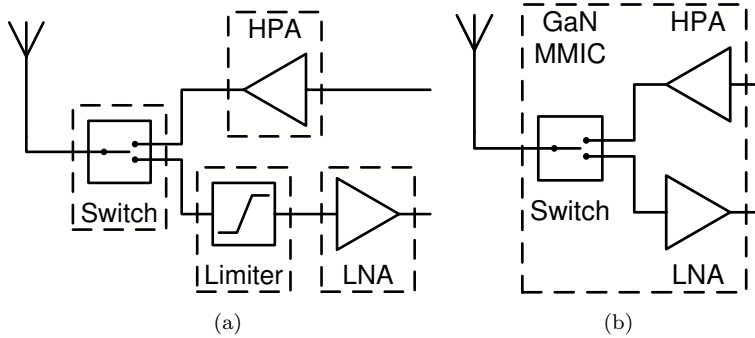


Figure 1.1: (a) Conventional multi-chip GaAs transceiver front-end. (b) Single-chip GaN transceiver front-end.

operating temperature of the LNA. Studies on cooled and heated GaN HEMTs have shown that the high frequency and low noise performance severely degrades with increasing temperature [21–23]. This is mainly due to the temperature dependence in the access resistances [A]. This has been verified by measuring the noise figure of a cooled LNA [24]. The noise figure was decreased with 0.3 dB, resulting in a sub 0.2 dB noise figure from 3–8 GHz at -30 °C. Accurate models, that take the self-heating into account are therefore needed to predict the performance of a GaN LNA. The low noise performance and its thermal dependence is studied and modeled in Chapter 3.

1.2 Wireless communications

Wireless communications systems such as radio base stations and microwave links could also benefit from GaN HEMT technology. This is due to the high peak efficiency and excellent linearity. Harmonically tuned power amplifiers have shown more than 80% power added efficiency (PAE) at 2 GHz [25]. While these harmonically tuned amplifiers achieve high peak efficiency (when driven deep into compression), their efficiency in back-off operation is poor. This is a problem for modulated communication signals such as W-CDMA with a peak to average power ratio of approximately 7 dB. This reduces the overall system efficiency, increasing the need for cooling the power amplifier.

There are several proposed solutions. Some of the most promising ones to increase the average efficiency are based on dynamic modulation of the transistor load impedance [26–28]. The idea behind load modulation is to control the output power in the most efficient way by synthesizing an optimum load impedance for a given input power. This enables substantial efficiency improvements for a modulated input signal. Load modulated high power amplifiers requires a controllable load network that withstands high powers. Load modulation networks employing SiC varactors as tuning elements is one promising solution [29].

In [28], a controllable load modulation network has successfully been implemented together with a power amplifier, improving the average efficiency. First a load-pull measurement was carried out on the PA to determine the optimum load trajectory. Then a controllable load network was designed, based

on voltage controlled varactors. The method relies on high efficiency amplifiers designed for $50\ \Omega$ systems, where the output matching network could limit the possibility to synthesize any arbitrary impedance. Thus measurements directly on a device would help in designing an optimum load modulation network. The load modulated PA is intended for use with modulated communications signals, hence the load needs to be dynamically controlled. Therefore a method is needed to characterize the transistor with a real communication signal at the input and a dynamically modulated load at the output. Such a system, allowing dynamic load modulation characterization at the device reference plane is described and verified in Chapter 4.

Chapter 2

Thermal measurements

The high power density of GaN HEMTs makes it possible to deliver more power from a smaller periphery transistor. The high power density could lead to larger self-heating, since a higher power is dissipated across a smaller surface area. The self-heating of a high power GaN HEMT could therefore significantly degrade its performance.

There is a large interest in using GaN MMIC circuits for high power and robust transceivers in airborne applications. These transceivers operate at elevated temperatures due to the high cost of efficient cooling and also due to the dissipated power in the HPA. The high temperature operation degrades the performance of the transmitter but in particular the sensitive receiver, where low noise operation is essential. Therefore both the self-heating and operation at elevated temperature are studied in this chapter.

2.1 Self-heating

The self-heating of transistors is determined by the dissipated dc power, the heat conductivity of the bulk material, and the thermal resistance of the package. The heat conductivity is determined by material properties and also the quality of the material growth [4]. Assuming linear heat transfer [30], the thermal resistance (R_{TH}) of the material is related to the channel temperature (T_{CH}):

$$T_{CH} = R_{TH}P_{diss} + T_A, \quad (2.1)$$

where T_A is the ambient temperature and P_{diss} is the dissipated dc power. The linear approximation of R_{TH} is only valid in a narrow temperature range and for small dissipated powers. In the general case, R_{TH} is temperature dependent [31].

Several methods are available to measure the channel temperature, for example electrical, Raman spectroscopy and infrared microscopy. The advantage with Raman spectroscopy is the very high resolution. Measurements have shown a steep temperature gradient within the active area for high dissipated power [32]. The downside is a time consuming measurement and special

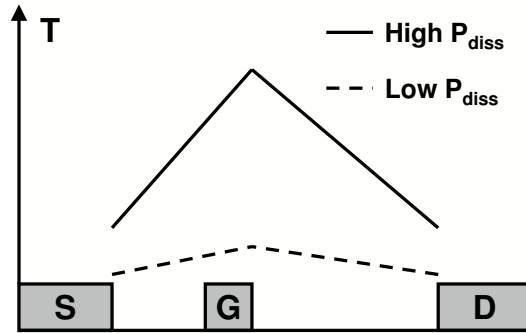


Figure 2.1: Schematic image over the temperature gradient within the active region of a GaN HEMT, according to [32].

mounting of the sample. Infrared measurements are fast and requires no special mounting, but the resolution is lower. In this thesis an IR microscope¹ with a pixel resolution of $1.6 \mu\text{m}$ ($800 \mu\text{m}/500$ pixels) is used for the self-heating measurements. The actual resolution is coarser, and at best $1.8 \mu\text{m}$ with the highest magnification. The spatial resolution limits the possibilities to resolve the temperature variations within the active area. However, it is shown in [32] that the temperature gradient is proportional to the dissipated powers, Fig. 2.1. Hence, for low dissipated power levels we can assume that the temperature gradient is small. The infrared image gives the average temperature in the measured pixel. For small temperature gradients, this corresponds to the channel temperature.

Measurements of R_{TH} are performed by controlling the dissipated power and measure the corresponding T_{CH} . The dissipated power is set by controlling V_{DS} and I_{DS} and is calculated as:

$$P_{diss} = V_{DS} \cdot I_{DS} \quad (2.2)$$

Infrared measurements of a $2 \times 100 \mu\text{m}$ GaN HEMT dissipating between 0.3 - 0.9 W are shown in Fig. 2.2. The self-heating of the active region is clearly visible.

The increase in T_{CH} due to dissipated power is measured at different ambient temperatures to study the influence of T_A . Infrared measurements showed no measurable dependence in R_{TH} versus ambient temperature in the temperature interval 323 - 373 K . The extracted R_{TH} is approximately 28 K/W , independent of T_A . The measured results are shown in Fig. 2.3, where the lines are modeled using (2.1), thus verifying the linear simplification.

2.2 Access resistances

The access resistances are directly related to the electron mobility of the material. In [7], a large temperature dependence of the electron mobility in GaN was shown. Therefore, it is important to characterize the access resistances

¹Infrascopie III, Quantum Focus Instruments

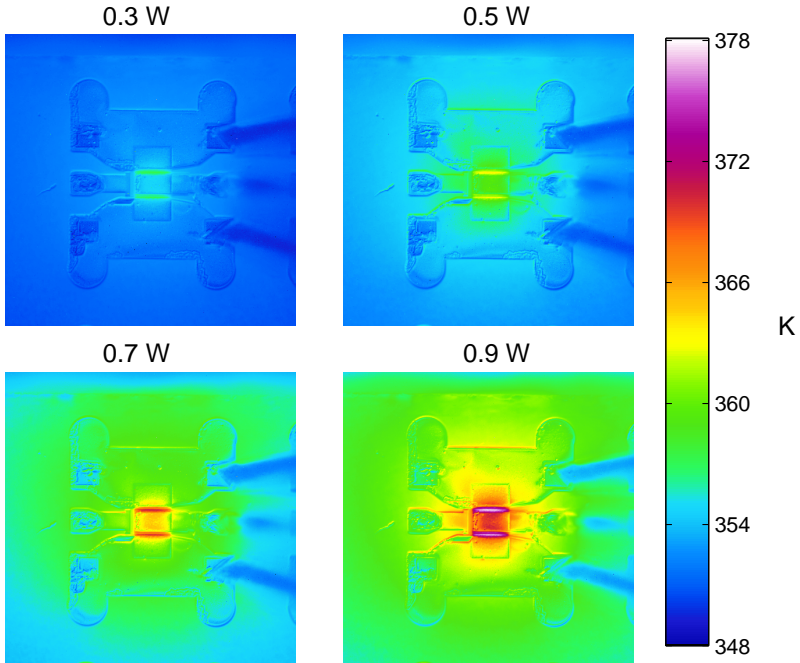


Figure 2.2: Infrared measurements of the increase in channel temperature for dissipated powers between 0.3-0.9 W with $T_A = 348$ K.

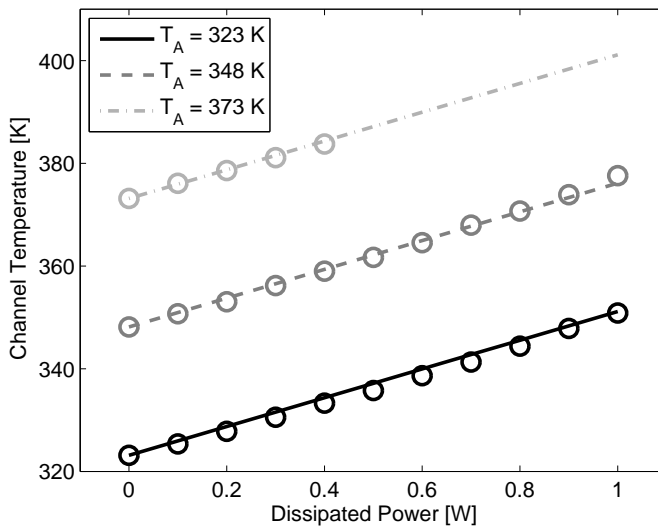


Figure 2.3: Increase in channel temperature due to dissipated dc-power for ambient temperatures between 323-373 K. Circles are measurements and the lines are computed from (2.1).

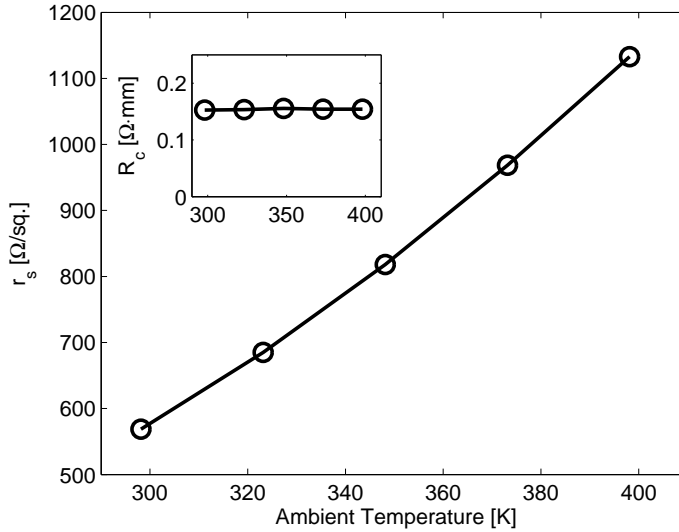


Figure 2.4: Extracted sheet resistivity r_s and ohmic-contact resistivity R_c for temperatures between 298-398 K.

temperature dependence to correctly take this into account when deriving models for high power transistors with large self-heating.

There are two parameters that determine the access resistance values, the ohmic-contact resistivity (R_c) and sheet resistivity (r_s). R_c is a process parameter related to the quality of the ohmic contacts and r_s is a material parameter related to the material growth and composition. These two parameters are extracted by performing a transfer length method (TLM) measurement, in which the resistances of the material and two contacts are measured for different contact separations [33]. The contribution from the contacts is constant for the different distances while the sheet resistance increases linearly. TLM measurements are carried out at ambient temperatures between 298-398 K to study the temperature dependence of R_c and r_s . The extracted contact resistivity is constant with temperature while the sheet resistivity increases quadratically, Fig. 2.4.

This indicates that a large temperature dependence in the access resistances is expected. Therefore, S-parameter measurements on a $2 \times 100 \mu\text{m}$ GaN HEMT are performed at ambient temperatures between 298-398 K to derive the dependence. The cold-FET method is used to extract the access resistances [34]. This method should be independent of self-heating since all measurements are made on a cold transistor ($V_{DS} = 0 \text{ V}$). The temperature dependence of the extracted access resistances is shown in Fig. 2.5.

The gate resistance (R_G) is independent of temperature since this is mainly a metallic resistance. Both the source resistance (R_S) and the drain resistance (R_D) increases with temperature as expected from the TLM measurements. The increase for R_S is 0.71 %/K and R_D increases with 0.86 %/K. The difference in gradients is due to the placement of the gate. The gate-drain distances for this device is $2 \mu\text{m}$ and the gate-source distance is $1 \mu\text{m}$. The TLM mea-

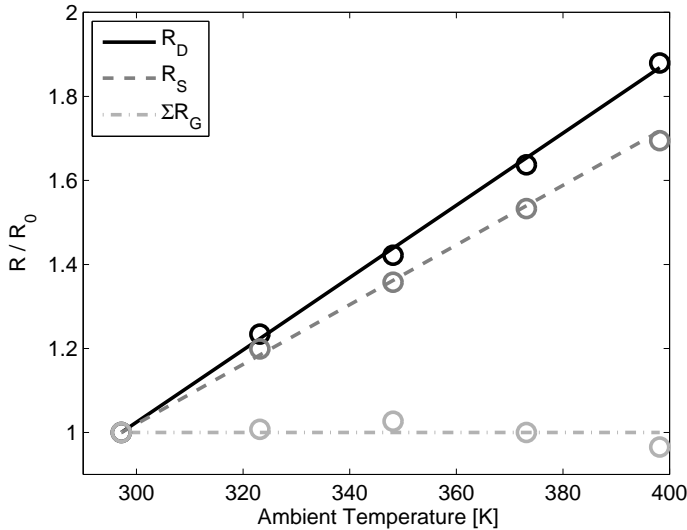


Figure 2.5: Normalized temperature dependence of the access resistances. Circles are measurements and the lines model the extracted dependence.

measurements concluded that only the sheet resistivity is temperature dependent. Therefore, longer distances, such as for the gate-drain distance, should show larger temperature dependence than shorter distances, since the sheet resistivity part on the total resistance is larger. The temperature dependent access resistances will, due to the self-heating, influence the extraction of the intrinsic small-signal parameters.

2.3 Intrinsic model parameters

The common procedure when extracting small-signal model parameters is to use some direct extraction method [35]. These methods assume that the extrinsic parameters are bias independent and therefore kept constant throughout the extraction. The self-heating studied in section 2.1 together with the temperature dependence seen in section 2.2 shows that this assumption is not valid for high power GaN HEMTs. Thus, the access resistances need to be corrected for their temperature dependence.

The access resistances influence on the extraction of the intrinsic parameters is illustrated for the intrinsic transconductance (g_m). It is given by the extrinsic transconductance G_m and R_S according to:

$$g_m = \frac{G_m}{1 - G_m R_S(T_{CH})} \quad (2.3)$$

where $R_S(T_{CH})$ is corrected for the self-heating. It is well known that extrinsic G_m decreases with temperature due to the decrease in electron mobility, while R_S is increasing. This results in a g_m that is less sensitive to temperature variations. The explanation is that, for short gate lengths, the current is de-

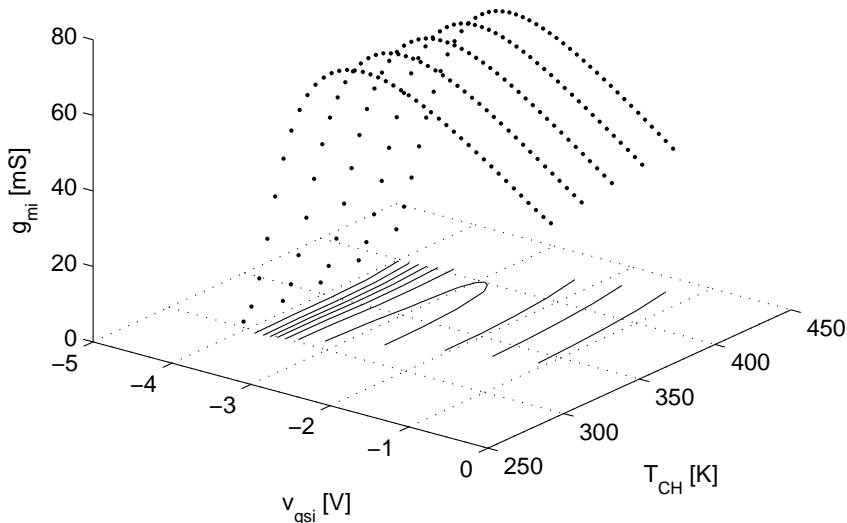


Figure 2.6: Intrinsic transconductance g_m versus channel temperature T_{CH} and intrinsic gate-source voltage v_{gsi} for a $2 \times 100 \mu\text{m}$ GaN HEMT at $V_{DS} = 9 \text{ V}$. Contours show 10 - 70 mS in 10 mS steps.

terminated by the electron saturation velocity instead of the electron mobility. The electron saturation velocity have been measured at different temperatures in [23, 36], showing a very small temperature dependence. It is therefore expected that the intrinsic g_m should have a small temperature dependence. The intrinsic g_m is extracted from the S-parameter measurements by taking into account both self-heating and the temperature dependent access resistances, shown in Fig. 2.6. A comparison between the extracted g_m with the new method and the standard method with constant R_S and R_D is shown in Fig. 2.7.

The contour lines for the new method are almost parallel with the temperature axis, indicating a very small temperature dependence for the intrinsic g_m . This effect is very clear for small dissipated power, while for large dissipated powers a small divergence in the contour lines is seen. This could be due to a temperature dependence in R_{TH} that was not observed in the extraction, or an underestimation of R_{TH} . Another explanation is the small temperature dependence observed in the electron saturation velocity. The standard method with constant R_S and R_D show a large temperature dependence for g_m .

The importance of taking the temperature dependence in the access resistances into account is further illustrated by studying the intrinsic S-parameters [B]. These are compared at two different ambient temperatures (297 K and 398 K) while keeping I_{DS} constant at 35 mA. The difference is large, and the intrinsic parameters show only a small temperature dependence when the ac-

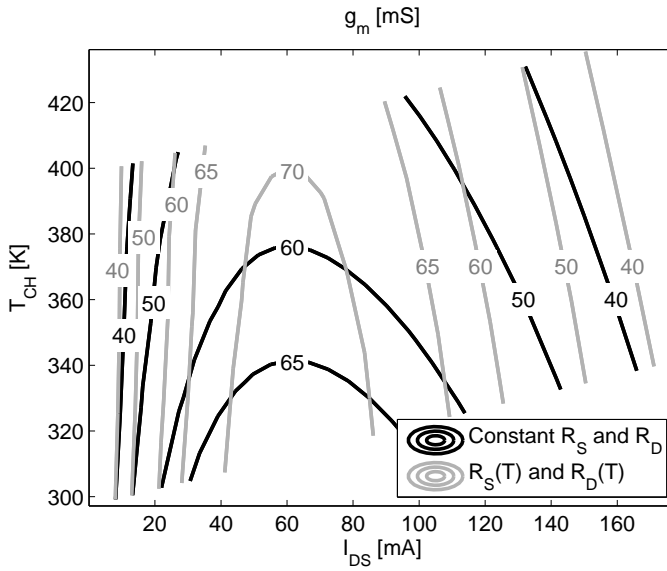


Figure 2.7: Comparison between the extracted g_m using the proposed method and the standard method with constant R_S and R_D .

cess resistances are corrected for their true value at the operating temperature, Fig. 2.8.

This indicate that most of the performance degradation at elevated temperatures is due to the temperature dependence in the access resistances. The proposed extraction method should simplify large signal modeling of high power GaN HEMTs.

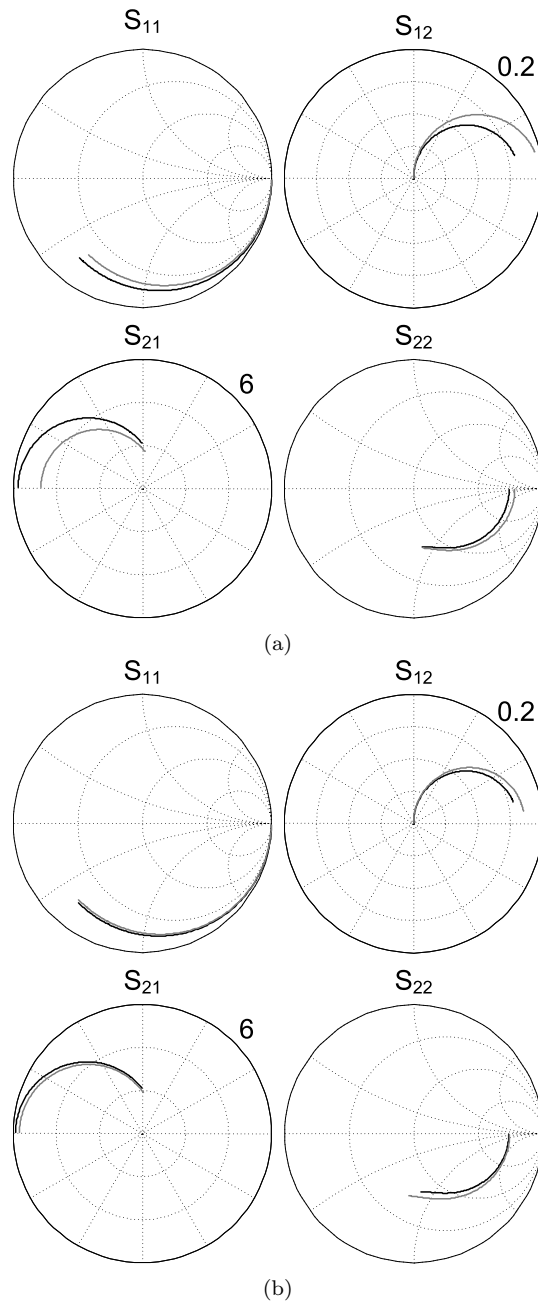


Figure 2.8: Intrinsic S-parameters for a $2 \times 100 \mu\text{m}$ GaN HEMT with $I_{DS} = 35 \text{ mA}$ at 297 K (black) and 398 K (gray). (a) R_S and R_D are kept constant with T_{CH} , (b) R_S and R_D are corrected for their temperature dependence.

Chapter 3

Noise characterization and modeling

As pointed out in Chapter 1, the GaN HEMT is a suitable candidate for airborne electronics due to the possibility to make small and light weight single-chip transceivers. One issue with this solution is that the receiver part, designed for very low noise, is working at elevated temperature. This results in an increase in the added thermal noise in all lossy parts and will also degrade the performance of the receiver due to the temperature dependence in material parameters seen in Chapter 2. Therefore, a temperature dependent noise model is needed to correctly predict the performance.

3.1 Noise parameter characterization

The added noise from a passive element can be calculated from the elements Z -parameters and the knowledge of the operating temperature. However, there is no analytical solution for the added noise from an active element. Therefore, the added noise from active elements needs to be measured to derive accurate models. The added noise from a two-port is given by its noise parameters according to:

$$F = F_{MIN} + \frac{4R_N}{Z_C} \frac{|\Gamma_{OPT} - \Gamma_S|^2}{|1 + \Gamma_{OPT}|^2 (1 - |\Gamma_S|^2)}, \quad (3.1)$$

F_{MIN} is the minimum noise figure. Γ_{OPT} is the optimum source impedance which gives F_{MIN} . R_N is the equivalent noise resistance, indicating how fast the noise figure is increased when the input is not matched to Γ_{OPT} . The noise parameters are measured using a tuner providing different source terminations (Γ_S) distributed across the Smith chart. By measuring the added noise power for at least four different source terminations it is possible to calculate the noise parameters of an active device. For higher accuracy more source impedances should be used.

The noise parameters of a 2x100 μm GaN HEMT fabricated in the in-house MMIC process have been measured [D]. It shows good low noise performance

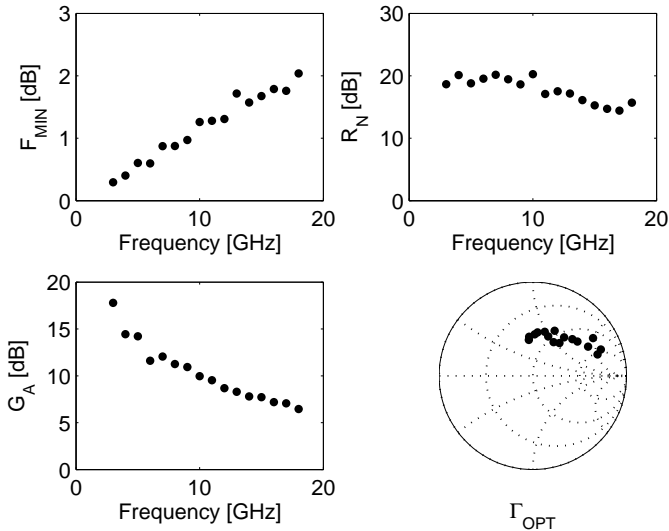


Figure 3.1: Measured noise parameters for a $2 \times 100 \mu\text{m}$ GaN HEMT with $V_{GS} = -2.25 \text{ V}$ and $V_{DS} = 6 \text{ V}$.

with F_{MIN} less than 2 dB up to 18 GHz. Typical noise parameters are shown in Fig. 3.1.

The temperature dependence of the noise parameters is studied by performing measurements at ambient temperatures between 297-398 K. The contribution from the temperature dependent access resistances is de-embedded following the procedure in [37]. The added intrinsic noise is significantly lower than the measured extrinsic noise. This concludes that the access resistances are the major contributors to the added noise. A degradation in noise performance with temperature is also observed, Fig. 3.2.

3.2 Noise modeling

The results in section 3.1 shows a large degradation in the noise performance due to the contribution from the access resistances. Even with the access resistances de-embedded there is a temperature dependence in the intrinsic noise parameters. This dependence needs to be modeled to predict the performance of a LNA operating at elevated temperature, such as in a high power transceiver. The proposed model is a small-signal model with two correlated noise current sources in shunt with the intrinsic HEMT, Fig. 3.3.

The access resistance are temperature dependent and adds thermal noise in the model. The noise contribution from the intrinsic resistances are included in the noise current sources. The intrinsic noise current sources are calculated from the de-embedded intrinsic noise parameters according to [38]:

$$\mathbf{C}_Y = \mathbf{T}\mathbf{C}_A\mathbf{T}^\dagger \quad (3.2)$$

where \mathbf{C}_Y is the admittance noise correlation matrix corresponding to a noise

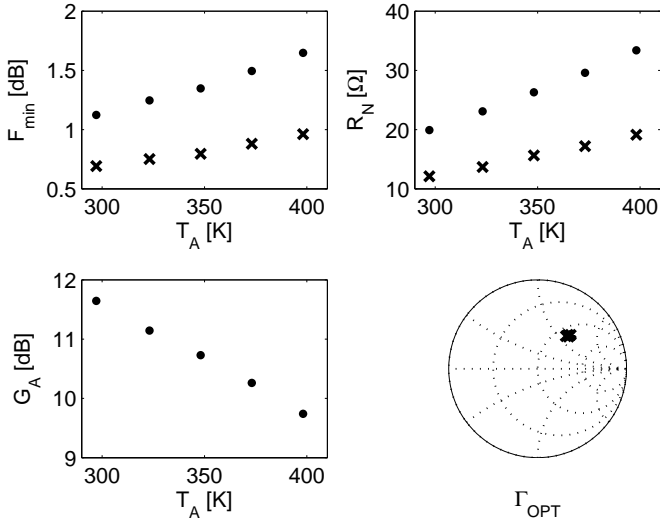


Figure 3.2: Measured temperature dependence of the noise parameters for a $2 \times 100 \mu\text{m}$ GaN HEMT at 9 GHz and $V_{DS} = 9 \text{ V}$ with $I_{DS} = 0.15 \cdot I_{DSS}$. Dots are measured noise parameters and crosses are de-embedded intrinsic noise parameters.

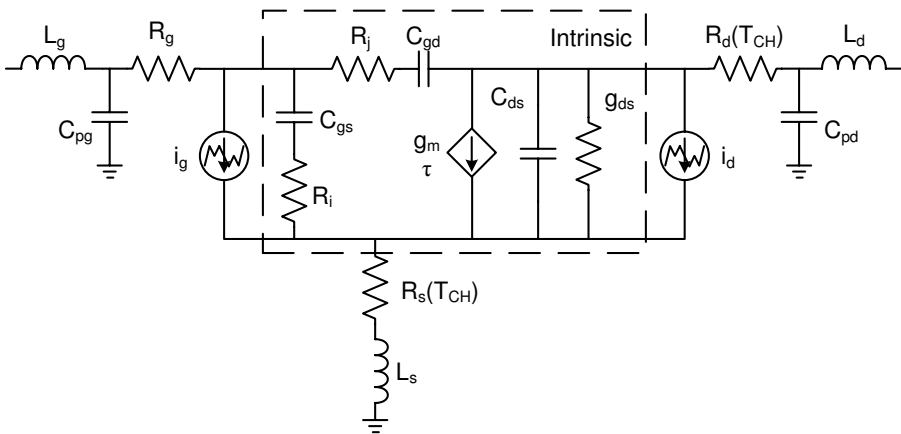


Figure 3.3: The small-signal noise model with two noise current sources and temperature dependent access resistances.

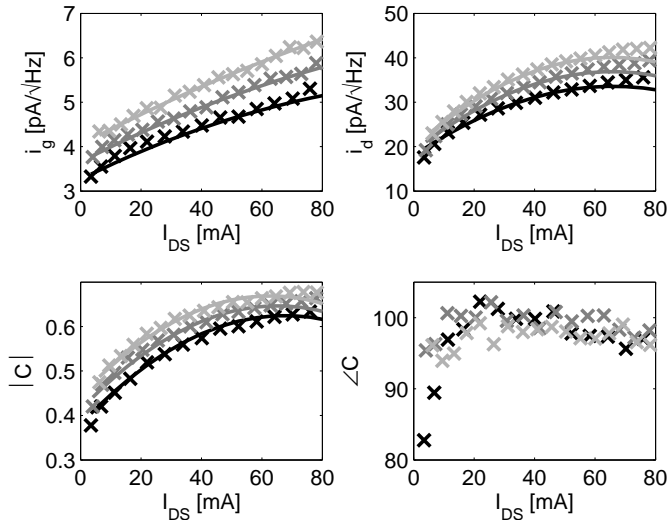


Figure 3.4: Extracted (cross) and modeled (line) noise current sources and their correlation coefficient for a $2 \times 100 \mu\text{m}$ GaN HEMT at 9 GHz and $V_{DS} = 9 \text{ V}$ at 297 K (black), 348 K (gray) and 398 K (lightgray)

current source representation:

$$\mathbf{C}_Y = \begin{bmatrix} i_g i_g^* & i_g i_d^* \\ i_d i_g^* & i_d i_d^* \end{bmatrix} \quad (3.3)$$

\mathbf{T} is a transformation matrix given by the Y-parameters of the intrinsic two-port:

$$\mathbf{T} = \begin{bmatrix} -Y_{11} & 1 \\ -Y_{21} & 0 \end{bmatrix} \quad (3.4)$$

\mathbf{C}_A is the chain noise correlation matrix derived from the noise parameters

$$\mathbf{C}_A = \begin{bmatrix} R_N & \frac{F_{MLN}-1}{2} - R_N Y_{OPT}^* \\ \frac{F_{MLN}-1}{2} - R_N Y_{OPT} & R_N |Y_{OPT}|^2 \end{bmatrix} \quad (3.5)$$

Y_{OPT} is the admittance representation of Γ_{OPT} . The correlation coefficient between the gate (i_g) and drain (i_d) noise current sources is given by:

$$C = \frac{\langle i_g i_d^* \rangle}{\sqrt{\langle i_g^2 \rangle \langle i_d^2 \rangle}} \quad (3.6)$$

The temperature and bias dependence for the noise current sources and their correlation coefficient is modeled, and the procedure is given in detail in [A]. The model agrees well with the extracted i_g , i_d and their correlation coefficient C , Fig. 3.4.

The frequency dependence of the small-signal noise model is verified at room temperature. The agreement between measured noise parameters and the simulation is good in the measured frequency range 3-18 GHz, Fig. 3.5.

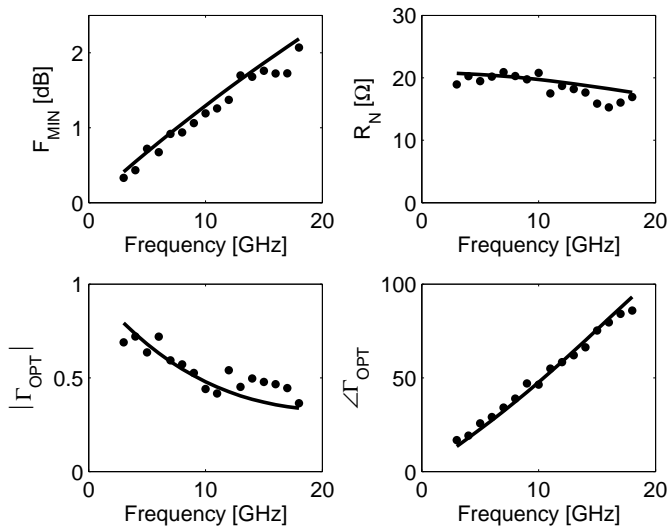


Figure 3.5: Measured (dots) and modeled (line) noise parameters for a 2x100 μm GaN HEMT at 9 GHz and $V_{DS} = 9$ V at room temperature

The proposed model is also verified for a fabricated MMIC amplifier. It is a resistive feedback amplifier intended for use in the IF chain in a complete transceiver solution. Measurements of the noise figure and gain are performed with a noise figure analyzer and compared to simulated results. The agreement is good as seen in Fig. 3.6.

3.3 Design of robust LNA

A main advantage with using GaN compared to GaAs is the increased robustness for high input powers. This could allow the removal of the limiter, or at least remove or simplifying some of the limiter stages. The limiter is lossy, thus it increases the overall noise performance of the receiver. Therefore, even if the noise figure of a GaAs LNA is lower compared to that of a GaN LNA, the overall system noise figure could be lower for a robust GaN receiver.

Large signal measurements are carried out on a 4x100 μm GaN HEMT to determine its robustness. The measurements shows that the GaN HEMT withstands a gate-source swing between -25 V and 7 V, while typical GaAs HEMTs withstand a voltage swing up to 11 V [17]. A large increase in the forward gate current is also seen due to the turn on of the gate diode, Fig 3.7.

The large gate current damages the material, thus degrading the performance of the LNA. This breakdown process was also shown in [9] where a gate resistor is suggested as a protective element. This resistor is placed in the gate bias feed, it cause a voltage drop, pinching the transistor when a large positive gate current is feed through it.

The proposed idea in [9], with a resistor in the bias feed is implemented in a one stage LNA. The LNA is designed to withstand high delivered input

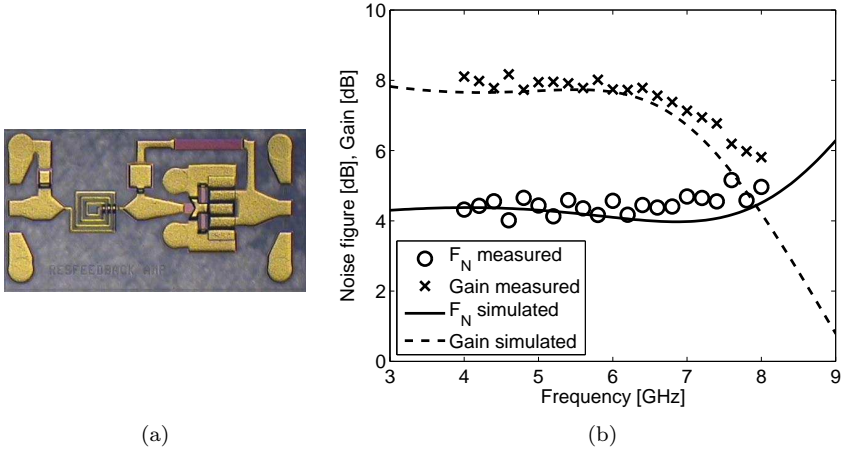


Figure 3.6: (a) Resistive feedback amplifier. (b) Simulated and measured noise figure and gain of the amplifier.

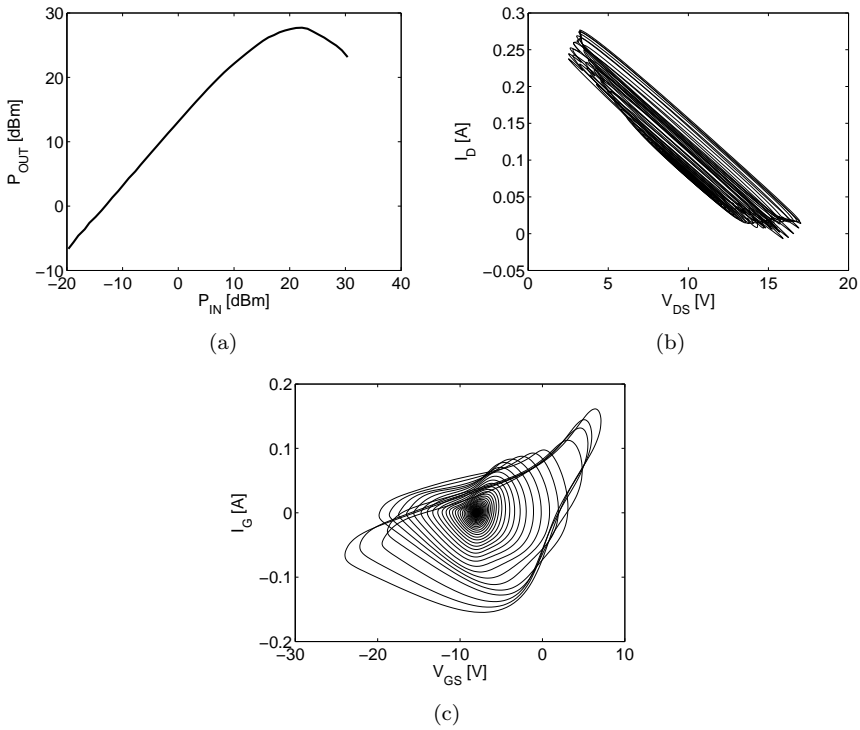


Figure 3.7: (a) Power sweep on a $4 \times 100 \mu\text{m}$ GaN HEMT with 50Ω termination at both input and output, (b) the corresponding voltage and current waveforms at the output, and (c) the corresponding voltage and current waveforms at the input.

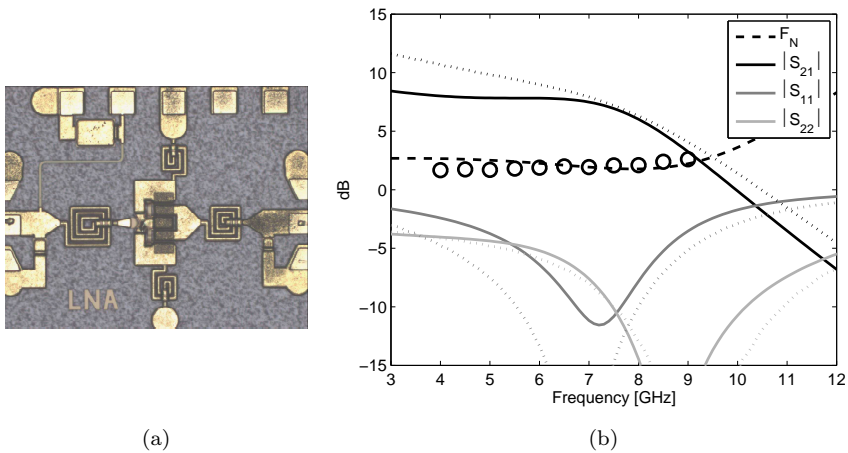


Figure 3.8: (a) Low noise amplifier designed for robustness. (b) Simulated (line) and measured (dotted) S-parameters together with simulated (dashed) and measured (circles) noise figure of the LNA.

powers, and a narrow band matching is used at a center frequency of 7.5 GHz. The simulation show a flat gain of more than 7 dB up to 7.5 GHz with a noise figure lower than 2 dB at the center frequency. S-parameter and noise parameters measurements have been carried out. The simulated matching and thus the gain of the LNA does not agree with the measured, Fig. 3.8 This is due to a problem with the inductor models in the MMIC design kit.

The measured noise figure agrees well with the simulated around the center frequency, but it is well below the simulated at lower frequencies. This is due to the increased gain at lower frequencies as a result of the incorrect inductor model. A survivability study have not yet been carried out to verify the increase in robustness due to the gate resistor.

Chapter 4

Dynamic load-pull

A common measurement for high power characterization of transistors is the load-pull measurement [39]. Different combinations of source and load impedances are synthesized at the transistors terminals using mechanical tuners. This gives insight about the optimum load impedances and also the expected performance from an amplifier circuit.

By combining tuners with a large signal network analyzer (LSNA), it is possible to measure the voltage and current waveforms at the device terminals. This improves the insight into device operation and increases modeling accuracy. The output data from a LSNA is the complex valued voltage and current phasors at all calibrated harmonics with a common phase reference. The voltages and currents are easily transformed into the load impedance seen by the DUT at each harmonic, opening up the possibility to perform load-pull also at the higher order harmonics, improving the performance of the DUT. There are commercial systems available based on mechanical tuners offering this possibility¹. The performance of all such systems is limited by the losses between the tuner and the DUT, since the tuner reflects the outgoing wave to synthesize the load.

This limitation is possible to overcome by using an active load [40]. In an active setup, the outgoing wave is terminated in a matched load. An amplitude and phase controlled wave is then injected towards the DUT to synthesize the load. An active setup, as long as the amplitude of the injected signal is high enough, has no problem in covering the entire Smith chart.

4.1 Active load-pull setup

The active system presented in this thesis is based on an open-loop architecture, allowing full control over the injected signal [C]. This type of system is not as prone to oscillation problems as some other types of active load pull systems based on a closed-loop architecture [41]. A LSNA² is used to sample the voltage waves a_1 , b_1 , a_2 and b_2 at the DUTs reference plane for the wanted number of harmonics. The input signal is generated with a Vector Signal Gen-

¹Multi-Purpose tuner, Focus Microwaves

²Maury/NMDG MT4463

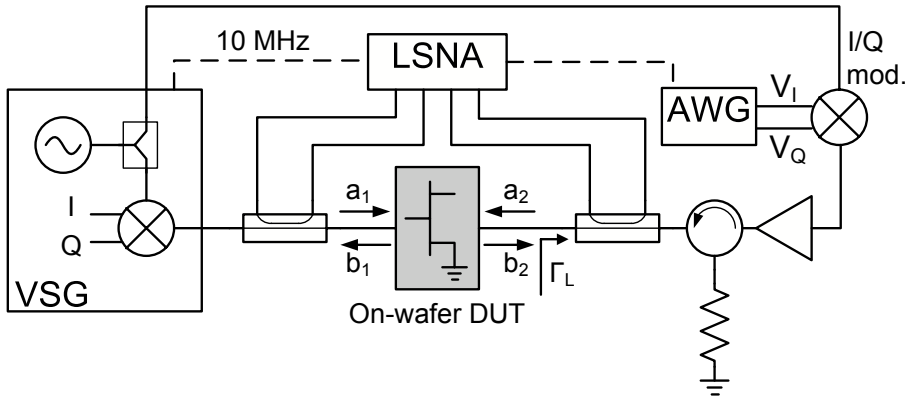


Figure 4.1: Active dynamic load-pull setup.

erator (VSG), allowing modulated input signals. The measurement setup is presented in Fig. 4.1.

The available input power, P_{IN} , delivered output power, P_{OUT} , and drain efficiency, η , are related to the measured voltage waves as follows:

$$P_{IN} = \frac{|a_1|^2}{2Z_0} \quad (4.1)$$

$$P_{OUT} = \frac{|b_2|^2 - |a_2|^2}{2Z_0} \quad (4.2)$$

$$\eta = \frac{P_{OUT}}{P_{DC}} \quad (4.3)$$

Drain efficiency is used as a measure of efficiency since no source pull is performed. The load reflection coefficient, Γ_L , is given by:

$$\Gamma_L = \frac{a_2}{b_2} \quad (4.4)$$

where

$$a_2 = A(V_I, V_Q) e^{j(\omega_0 t + \phi(V_I, V_Q))} \quad (4.5)$$

The injected a_2 wave is synthesized with an IQ-modulator to control its amplitude and phase. Where the control voltages V_I and V_Q to the modulator are controlled using an Arbitrary Waveform Generator (AWG). It is therefore possible to dynamically control a_2 with a predetermined control scheme.

4.2 Load modulation

Modulation schemes such as W-CDMA, used for wireless communication have a large amplitude variation in the output signal. Thus the amplifier works approximately 7 dB below the peak output power most of the time. The performance in back-off is not optimal since the amplifier needs to be designed for the peak output power, resulting in lower average efficiency.

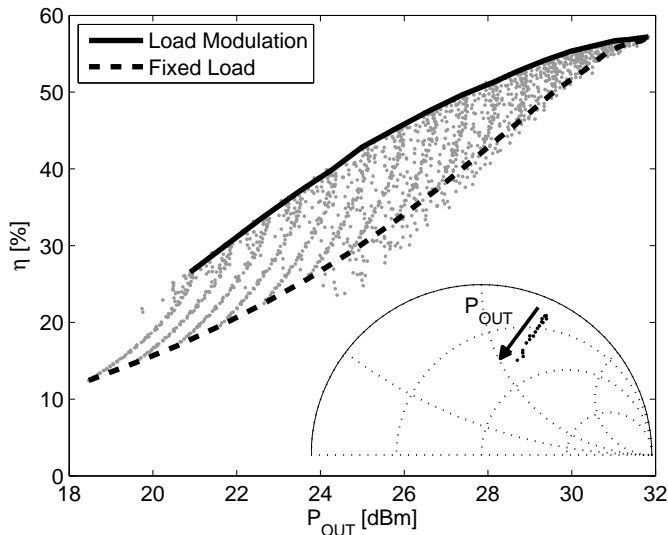


Figure 4.2: Static characterization of load modulation.

One promising method of improving the efficiency in back-off operation is load modulation [27]. The idea behind load modulation is to change the load with the envelop of a modulated input signal. By changing the load in an optimum way it is possible to increase the efficiency in back-off operation [28]. Therefore a static load-pull characterization is first performed on the used transistor to determine the optimum way of controlling the load reflection coefficient. The static characterization is performed by sweeping the input power and at each input power performing a load-pull measurement. These measurement gives the optimum Γ_L as a function of output power that corresponds to the highest efficiency.

In this study a $10 \times 300 \mu\text{m}$ laterally diffused metal oxide semiconductor (LDMOS) is used, but the characterization procedure is technology independent. The input power is swept from 5 to 22 dBm in 1 dB steps and load-pull is performed at each input power using the active injection based setup. The measured optimum Γ_L trajectory together with the improvement in efficiency compared to a fixed load versus output power is seen in Fig. 4.2.

4.3 Dynamic load modulation characterization

The dynamic load modulation characterization setup is verified by using a modulated input signal, thus a time varying output power. The time varying output signal is synthesized with an amplitude modulated three tone multisine signal. The dynamic range of the signal is chosen to 10 dB, compared with the peak to average of 7 dB for a W-CDMA signal. The modulated input signal is then calculated from the generated three tone and knowledge about the distortion in the DUT.

Γ_L is controlled with an AWG that is synchronized with the VSG providing

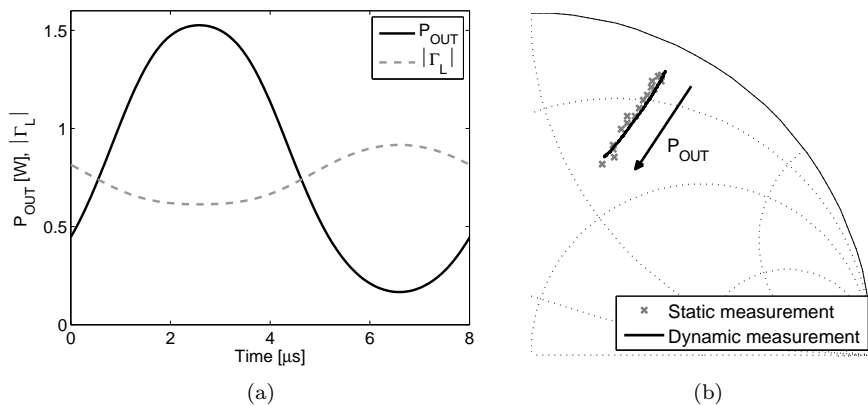


Figure 4.3: (a) The time varying output power and magnitude of the reflection coefficient. (b) The time varying load compared with the static characterization.

the input signal. The static characterization of the used LDMOS showed that the control voltages V_I and V_Q were approximately constant with output power. This is explained by the optimum load trajectory in Fig. 4.2 and the definition of Γ_L in equation (4.4). The trajectory follows a straight line, thus the magnitude of Γ_L is decreasing with output power. This is obtained by using a constant a_2 wave if the decrease in $|\Gamma_L|$ is proportional to the increase in $|b_2|$.

The measured time varying delivered output power together with the time varying magnitude of Γ_L are shown in Fig. 4.3a. In Fig. 4.3b, the time varying Γ_L is compared with the optimum trajectory obtained from the static load-pull characterization.

The measured time varying $|\Gamma_L|$ is decreasing with increased output power, in accordance with the static characterization. The agreement between measured dynamic Γ_L and the optimum trajectory obtained in the static characterization is excellent. This verifies the dynamic characterization, opening new possibilities for device level characterization aimed for high efficiency amplifier design. This could help in the design of integrated controllable load networks, further improving the efficiency.

An interesting application of the presented characterization setup could be in the design of Doherty power amplifiers. The Doherty amplifier works in a way where two amplifiers perform load pull on each other. This makes it very difficult to study the operation of the transistors in the two amplifiers separately. By controlling the load with the AWG and the IQ modulator properly it is possible to use the proposed characterization setup to simulate this environment at the device level and test the suitability of devices for Doherty amplifier application with modulated signals.

Chapter 5

Conclusions

The GaN HEMT has shown to be a very promising semiconductor technology for many applications, such as high efficiency power amplifiers, linear high power amplifiers and multi octave high power amplifiers. Due to the high electron mobility, it is also very promising for robust low noise receivers. The high output power together with the promising low system noise figure makes the GaN HEMT MMIC technology very interesting for robust high power transceivers for radar applications.

The high power density combined with smaller periphery could lead to new thermal considerations for high power amplifiers. The thermal properties has thoroughly been investigated in Chapter 2. The self-heating was measured using an IR-microscope, resulting in a thermal resistance of 28 K/W. The temperature dependence of the access resistances was also studied, showing a large increase with temperature. This was also verified with TLM measurements. The extracted g_m shows only a weak temperature dependence when the temperature dependence of the access resistances is taken into account in the model parameter extraction. The small temperature dependence seen in g_m could possibly simplify large signal modeling. These temperature effects, which are usually overlooked, are important and should be implemented in the small-signal and large-signal models to correctly predict the performance of the GaN HEMT.

In this thesis, a new advanced active load-pull characterization method was also presented. The load can be dynamically controlled allowing dynamic load modulation characterization directly at the transistor level in a probe station or fixture. The method opens up new possibilities for investigating the device behavior and for designing load modulated power amplifiers with increased efficiency in back-off operation.

5.1 Future work

The GaN HEMT is a very promising technology for single-chip radar transceivers. But there has still not been published a fully integrated GaN transceiver. This is of large interest, allowing comparison of system performance between GaN and GaAs. The GaN MMIC fabrication line at Chalmers have shown the possibility of fabricating all the circuits needed for a complete transceiver. It is a

matter of step by step increasing the integration factor. Such a system level comparison is necessary to fully demonstrate the potential of the GaN HEMT.

The self-heating studied in Chapter 2 raised some questions regarding the current transport in GaN. Further investigation considering the electron saturation velocity is needed. How large is the temperature dependence, and is it possible to assume that all temperature dependence is in the access resistances? Further investigation is needed for higher dissipated powers, since R_{TH} is expected to be temperature dependent, thus power dependent. This behavior was not observed for the low dissipated powers in this thesis.

It should be very interesting to perform the thermal characterization on other materials to compare. It is well known that the transconductance for GaAs show a large temperature dependence. Is this due to material parameters or is the current dependent on the mobility to a larger extent than on electron saturation velocity.

The dynamic load modulation setup in Chapter 4 show some interesting applications. It could be used to improve the design of load modulated amplifiers, for example designing power amplifiers with integrated load modulation network. It also makes it possible to characterize the intrinsic waveforms of a Doherty amplifier by measuring on one path at a time, simulating the load modulation due to the other amplifier.

Acknowledgment

This work would never have happened without the help and support from several persons. Therefore I would like to express my gratitude to those who have supported my work.

First I would like to thank my examiner Prof. Herbert Zirath for giving me the opportunity to work and perform research at the Microwave Electronics Laboratory.

I would like to express my greatest thank to my co-supervisor Kristoffer Andersson for his endless support and encouragement. He has guided me into the world of research and he has always had the time for discussions and proof reading.

My supervisor Niklas Rorsman for his support, guidance and endless work in the clean room to fabricate the GaN HEMTs and MMICs.

I am really thankful to the director of the GigaHertz Centre, Prof. Jan Grahn for creating a great environment to carry out research in close collaboration with world leading companies in the microwave electronics industry.

I would like to thank the entire wide bandgap group for the great support. Whose work in the clean room is of greatest importance for my research. Keep up the good work!

Christian Fager for fruitful discussions and introducing me to the world of modulated signals and measurements.

Itcho Angelov for proof reading and interesting discussion concerning measurements and modeling.

I would also like to thank Hans Hjelmgren for proof reading this thesis.

This research has been carried out in the GigaHertz Centre in a joint research project financed by the Swedish Governmental Agency of Innovation Systems (VINNOVA), Chalmers University of Technology and Saab AB.

Bibliography

- [1] U. Mishra, S. Likun, T. Kazior, and Y.-F. Wu, “GaN-Based RF Power Devices and Amplifiers,” *Proceedings of the IEEE*, vol. 96, no. 2, pp. 287–305, Feb. 2008.
- [2] [Online]. Available: <http://www.ioffe.rssi.ru/SVA/NSM/Semicond/>
- [3] Y.-F. Wu, M. Moore, A. Saxler, T. Wisleder, and P. Parikh, “40-W/mm Double Field-plated GaN HEMTs,” *Device Research Conference, 2006 64th*, pp. 151–152, June 2006.
- [4] G. J. Riedel, J. W. Pomeroy, K. P. Hilton, J. O. Maclean, D. J. Wallis, M. J. Uren, T. Martin, U. Forsberg, A. Lundskog, A. Kakanakova-Georgieva, G. Pozina, E. Janzen, R. Lossy, R. Pazirandeh, F. Brunner, J. Wurfl, and M. Kuball, “Reducing Thermal Resistance of AlGaN/GaN Electronic Devices Using Novel Nucleation Layers,” *Electron Device Letters, IEEE*, vol. 30, no. 2, pp. 103–106, Feb. 2009.
- [5] R. Quay, Ed., *Gallium Nitride Electronics*. Springer Berlin Heidelberg, 2008.
- [6] B. Green, H. Henry, J. Selbee, F. Clayton, K. Moore, M. CdeBaca, J. Abdou, C.-L. Liu, O. Hartin, D. Hill, M. Miller, and C. Weitzel, “Characterization and thermal analysis of a 48 V GaN HFET device technology for wireless infrastructure applications,” *Microwave Symposium Digest, 2008 IEEE MTT-S International*, pp. 651–654, June 2008.
- [7] I. Daumiller, C. Kirchner, M. Kamp, K. Ebeling, and E. Kohn, “Evaluation of the temperature stability of AlGaN/GaN heterostructure FETs,” *Electron Device Letters, IEEE*, vol. 20, no. 9, pp. 448–450, Sep 1999.
- [8] P. Parikh, Y. Wu, M. Moore, P. Chavarkar, U. Mishra, R. Neidhard, L. Kehias, and T. Jenkins, “High linearity, robust, AlGaN-GaN HEMTs for LNA and receiver ICs,” *High Performance Devices, 2002. Proceedings. IEEE Lester Eastman Conference on*, pp. 415–421, Aug. 2002.
- [9] M. Rudolph, R. Behtash, R. Doerner, K. Hirche, J. Wurfl, W. Heinrich, and G. Trankle, “Analysis of the Survivability of GaN Low-Noise Amplifiers,” *Microwave Theory and Techniques, IEEE Transactions on*, vol. 55, no. 1, pp. 37–43, Jan. 2007.

- [10] J. Janssen, M. van Heijningen, G. Provenzano, G. Visser, E. Morvan, and F. van Vliet, "X-Band Robust AlGa_N/Ga_N Receiver MMICs with over 41 dBm Power Handling," *Compound Semiconductor Integrated Circuits Symposium, 2008. CSICS '08. IEEE*, pp. 1–4, Oct. 2008.
- [11] M. Micovic, A. Kurdoghlian, H. Moyer, P. Hashimoto, A. Schmitz, I. Milosavljevic, P. Willadsen, W.-S. Wong, J. Duvall, M. Hu, M. Wetzel, and D. Chow, "Ga_N MMIC technology for microwave and millimeter-wave applications," *Compound Semiconductor Integrated Circuit Symposium, 2005. CSIC '05. IEEE*, pp. 3 pp.–, Oct.-2 Nov. 2005.
- [12] D. Krausse, R. Quay, R. Kiefer, A. Tessmann, H. Massker, A. Leuther, A. Merkle, S. Müller, C. Schwörer, M. Mikulla, M. Schlechtweg, and G. Weimann, "Robust Ga_N HEMT Low-Noise Amplifier MMICs for X-Band Applications," *Gallium Arsenide applications symposium. GAAS 2004, 11-12 October, Amsterdam*, pp. 71–74, Oct. 2004.
- [13] J. De Jaeger, S. Delage, G. Dambrine, M. Di Forte Poisson, V. Hoel, S. Lepilliet, B. Grimbert, E. Morvan, Y. Mancuso, G. Gauthier, A. Lefrancois, and Y. Cordier, "Noise assessment of AlGa_N/Ga_N HEMTs on Si or SiC substrates: application to X-band low noise amplifiers," *Gallium Arsenide and Other Semiconductor Application Symposium, 2005. EGAAAS 2005. European*, pp. 229–232, Oct. 2005.
- [14] M. Aust, S. A.K., C. Y.-C., and W. M., "Wideband Dual-Gate Ga_N HEMT Low Noise Amplifier for Front-End Receiver Electronics," *Compound Semiconductor Integrated Circuit Symposium, 2006. CSIC 2006. IEEE*, pp. 89–92, Nov. 2006.
- [15] K. Kobayashi, Y. C. Chen, I. Smorchkova, R. Tsai, M. Wojtowicz, and A. Oki, "A 2 Watt, Sub-dB Noise Figure Ga_N MMIC LNA-PA Amplifier with Multi-octave Bandwidth from 0.2-8 GHz," *Microwave Symposium, 2007. IEEE/MTT-S International*, pp. 619–622, June 2007.
- [16] R. Schwindt, V. Kumar, O. Aktas, J. Lee, and I. Adesida, "AlGa_N/Ga_N HEMT-based fully monolithic X-band low noise amplifier," *Physica Status Solidi Conferences*, vol. 2, pp. 2631–2634, 2005.
- [17] Y. Chen, M. Barsky, R. Tsai, R. Lai, H. Yen, A. Oki, and D. Streit, "Survivability of InP HEMT devices and MMICs under high RF input drive," *Microwave Symposium Digest., 2000 IEEE MTT-S International*, vol. 3, pp. 1917–1920 vol.3, 2000.
- [18] A. Maas, J. Janssen, and F. van Vliet, "Set of X-band distributed absorptive limiter GaAs MMICs," *Radar Conference, 2007. EuRAD 2007. European*, pp. 17–20, Oct. 2007.
- [19] S. Rosenbaum, C. Chou, C. Ngo, L. Larson, T. Liu, and M. Thompson, "A 7 to 11 GHz AlInAs/GaInAs/InP MMIC low noise amplifier," *Microwave Symposium Digest, 1993., IEEE MTT-S International*, pp. 1103–1104 vol.2, 1993.

- [20] P. Schuh, H. Sledzik, R. Reber, A. Fleckenstein, R. Leberer, M. Oppermann, R. Quay, F. van Raay, M. Seelmann-Eggebert, R. Kiefer, and M. Mikulla, "GaN MMIC based T/R-Module Front-End for X-Band Applications," *Microwave Integrated Circuit Conference, 2008. EuMIC 2008. European*, pp. 274–277, Oct. 2008.
- [21] S. Nuttinck, E. Gebara, J. Laskar, and M. Harris, "High-frequency noise in AlGaIn/GaN HFETs," *Microwave and Wireless Components Letters, IEEE*, vol. 13, no. 4, pp. 149–151, Apr 2003.
- [22] S. Nuttinck, B. Wagner, B. Banerjee, S. Venkataraman, E. Gebara, J. Laskar, and H. Harris, "Thermal analysis of AlGaIn-GaN power HFETs," *Microwave Theory and Techniques, IEEE Transactions on*, vol. 51, no. 12, pp. 2445–2452, Dec. 2003.
- [23] Nidhi, T. Palacios, A. Chakraborty, S. Keller, and U. Mishra, "Study of Impact of Access Resistance on High-Frequency Performance of Al-GaN/GaN HEMTs by Measurements at Low Temperatures," *Electron Device Letters, IEEE*, vol. 27, no. 11, pp. 877–880, Nov. 2006.
- [24] K. Kobayashi, Y. C. Chen, I. Smorchkova, B. Heying, W.-B. Luo, W. Sutton, M. Wojtowicz, and A. Oki, "A Cool, Sub-0.2 dB, Ultra-Low Noise Gallium Nitride Multi-Octave MMIC LNA-PA with 2-Watt Output Power," *Compound Semiconductor Integrated Circuits Symposium, 2008. CSICS '08. IEEE*, pp. 1–4, Oct. 2008.
- [25] D. Schmelzer and S. Long, "A GaN HEMT Class F Amplifier at 2 GHz With > 80% PAE," *Solid-State Circuits, IEEE Journal of*, vol. 42, no. 10, pp. 2130–2136, Oct. 2007.
- [26] S. Cripps, *RF power amplifiers for wireless communications, 2nd. ed.* Artech House, 2006.
- [27] F. Raab, "High-efficiency linear amplification by dynamic load modulation," *Microwave Symposium Digest, 2003 IEEE MTT-S International*, vol. 3, pp. 1717–1720 vol.3, June 2003.
- [28] H. Nemati, C. Fager, U. Gustavsson, R. Jos, and H. Zirath, "Design of varactor-based tunable Matching networks for dynamic load modulation of high power amplifiers," *Accepted for publication in Microwave Theory and Techniques, IEEE Transactions on*, 2009.
- [29] M. Südwow, H. Nemati, M. Thorsell, U. Gustavsson, K. Andersson, C. Fager, P.-Å. Nilsson, J. ul Hassan, A. Henry, E. Janzen, R. Jos, and N. Rorsman, "SiC Varactors for Dynamic Load Modulation of High Power Amplifiers," *Electron Device Letters, IEEE*, vol. 29, no. 7, pp. 728–730, July 2008.
- [30] H. Fukui, "Thermal resistance of GaAs field-effect transistors," *Electron Devices Meeting, 1980 International*, vol. 26, pp. 118–121, 1980.
- [31] A. M. Conway, P. M. Asbeck, J. S. Moon, and M. Micovic, "Accurate thermal analysis of GaN HFETs," *Solid-State Electronics*, vol. 52, no. 5, pp. 637–643, 2008.

- [32] R. Simms, J. Pomeroy, M. Uren, T. Martin, and M. Kuball, "Channel Temperature Determination in High-Power AlGa_N/Ga_N HFETs Using Electrical Methods and Raman Spectroscopy," *Electron Devices, IEEE Transactions on*, vol. 55, no. 2, pp. 478–482, Feb. 2008.
- [33] H. Berger, "Contact resistance on diffused resistors," *Solid-State Circuits Conference. Digest of Technical Papers. 1969 IEEE International*, vol. XII, pp. 160–161, Feb 1969.
- [34] G. Dambrine, A. Cappy, F. Heliodore, and E. Playez, "A new method for determining the FET small-signal equivalent circuit," *Microwave Theory and Techniques, IEEE Transactions on*, vol. 36, no. 7, pp. 1151–1159, Jul 1988.
- [35] N. Rorsman, M. Garcia, C. Karlsson, and H. Zirath, "Accurate small-signal modeling of HFET's for millimeter-wave applications," *Microwave Theory and Techniques, IEEE Transactions on*, vol. 44, no. 3, pp. 432–437, Mar 1996.
- [36] C. Oxley, M. Uren, A. Coates, and D. Hayes, "On the temperature and carrier density dependence of electron saturation velocity in an Al-GaN/GaN HEMT," *Electron Devices, IEEE Transactions on*, vol. 53, no. 3, pp. 565–567, Mar 2006.
- [37] R. Pucel, W. Struble, R. Hallgren, and U. Rohde, "A general noise de-embedding procedure for packaged two-port linear active devices," *Microwave Theory and Techniques, IEEE Transactions on*, vol. 40, no. 11, pp. 2013–2024, Nov 1992.
- [38] H. Hillbrand and P. Russer, "An efficient method for computer aided noise analysis of linear amplifier networks," *Circuits and Systems, IEEE Transactions on*, vol. 23, no. 4, pp. 235–238, Apr 1976.
- [39] J. Cusack, S. Perlow, and B. Perlman, "Automatic load contour mapping for microwave power transistors," *Microwave Theory and Techniques, IEEE Transactions on*, vol. 22, no. 12, pp. 1146–1152, Dec 1974.
- [40] Y. Takayama, "A New Load-Pull Characterization Method for Microwave Power Transistors," *Microwave Symposium Digest, MTT-S International*, vol. 76, no. 1, pp. 218–220, Jun 1976.
- [41] G. Bava, U. Pisani, and V. Pozzolo, "Active load technique for load-pull characterisation at microwave frequencies," *Electronics Letters*, vol. 18, no. 4, pp. 178–180, Feb 1982.

Paper A

Thermal Study of the High-Frequency Noise in GaN HEMTs

M. Thorsell, K. Andersson, M. Fagerlind, M. Südow, P.-Å. Nilsson,
and N. Rorsman

in *IEEE Transactions on Microwave Theory and Techniques*, vol. 57,
no. 1, pp. 19–26.

Paper B

Characterization of the temperature dependent access resistances in AlGa_N/Ga_N HEMTs

M. Thorsell, K. Andersson, M. Fagerlind, M. Südow, P.-Å. Nilsson, and N. Rorsman

in *2008 Workshop on Integrated Nonlinear Microwave and Millimetre-Wave Circuits*, Malaga, Spain, 2008, pp. 17–20.

Paper C

Characterization Setup for Device Level Dynamic Load Modulation Measurements

M. Thorsell, K. Andersson, and C. Fager

in *2009 IEEE MTT-S International Microwave Symposium Digest*, Boston, MA, USA, 2009.

Paper D

**An AlGa_N/Ga_N HEMT-Based Microstrip MMIC Process
for Advanced Transceiver Design**

**M. Südow, M. Fagerlind, M. Thorsell, K. Andersson, N. Billström,
P.-Å. Nilsson, and N. Rorsman**

**in *IEEE Transactions on Microwave Theory and Techniques*, vol. 56,
no. 8, pp. 1827–1833.**

